Journal of Hydraulic Research Vol. 44, No. 6 (2006), pp. 832–840

Resistance coefficient in a smooth concentric annular pipe

Coefficient de résistance dans une conduite annulaire concentrique lisse

MICHELE MOSSA, PhD, Professor, *IAHR Member, DIASS, Technical University of Bari, Via E. Orabona 4, 70125 Bari, Italy*

ABSTRACT
This paper reports an experimental study aimed at determining turbulence and resistance coefficient characteristics of the flow field in smooth concentric annular conduits. The measurements of velocity field were performed with a laser Doppler anemometer system in the flow region between the inner wall and the radius of maximum velocity (inner region). Velocity profiles along a vertical line normal to the walls are represented in terms of law of the wall. The maximum mean local velocity occurs at positions in agreement with literature formulae. For different distances from the inner wall micro and integral scales of turbulence were calculated. The results show that in flows with high Reynolds numbers small eddies tend to assume greater frequencies and that the time interval over which fluctuating velocity is correlated with itself becomes smaller. A statistical description of turbulence is also reported. The expression of the inner resistance coefficient was obtained by integrating the velocity law. The calculated resistance coefficients are in fair agreement with the experimental ones. Both are always greater than the corresponding values for circular conduits.

RÉSUMÉ
Ce présent article rapporte les résultats d'une étude expérimentale sur l'écoulement turbulent dans des conduits annulaires concentriques lisses, à partir d'une analyse de la turbulence et de la définition de la loi de résistance. La détermination des composantes longitudinales de la vitesse, dans la région du flux située entre le mur intérieur et le point ou l'écoulement rejoint une valeur maximale de sa vitesse locale moyenne, ont été effectuées par le biais d'un système LDA. La position du point, à la quelle la vitesse est maximale, est été confirmée, après comparaison, par les formules principales qui sont présentées en littérature. En outre, les micro et les grandes échelles de la turbulence ont été calculées. Ces derniers résultats montrent que; à l'augmentations du nombre de Reynold's de l'écoulement, les petits rouleaux tendent à présenter, toujours, avec des fréquence de valeur de plus en plus grandes, alors que l'intervalle du temps, durant la quelle les composantes fluctuantes de la vitesse sont corrélées avec elles-mêmes, tend à se réduire de plus en plus. Les analyses statistiques de la turbulence sont, aussi, représentés dans ce présent travail. A travers une intégration de la loi de la vitesse, obtenue expérimentalement, le coefficient de la résistance interne a été déterminé. Les coefficients de la résistance calculés sont comparables avec celles de l'expérimentation. Les deux sont, toujours, plus grands que celles détermines pour des conduites a section circulaire.

Keywords: Annular conduit, turbulence, eddies, law of the wall, resistance coefficient, fluid mechanics.

1 Introduction

The present paper reports an experimental study of turbulent flow in concentric smooth annular conduits.

The expression for the resistance coefficient (f) of turbulent flow in circular pipes cannot be applied to annular conduits, without taking into account the shape factor of the conduit cross section. In addition, there is a lack of experimental data regarding the characteristics of turbulence in annular conduits, although they are widely used in nuclear and chemical engineering applications (Gentilini, 1935; Ghetti, 1950; Jonsson and Sparrow, 1966; Rothfus *et al.*, 1966; Quarmby, 1967; Melling and Whitelaw, 1976; Sharma *et al.*, 1976; Shands *et al.*, 1980; Greco and Pulci Doria, 1983; Cardoso *et al.*, 1989; Mossa, 1991; Idelchik, 1994).

From extensive studies of turbulent flows in smooth circular conduits, it was found that velocity near the wall follows a universal relation called the *law of the wall*. This law was found to be valid in different types of conduits as well as in open channels. In the outer layer the velocity profiles deviate from the *logarithmic law*. Coles (1956) extended the law of the wall by adding a purely empirical function called *wake function* in order to express the entire profile. A similar function was proposed by Marchi (1961).

The present experimental study investigates the velocity distributions in turbulent flow through a smooth annular conduits. Longitudinal velocity components were measured at many points along a vertical radius using a laser Doppler anemometer (LDA) system (Durst *et al.*, 1976; Lamberti *et al.*, 1983; Cenedese *et al.*, 1990).

Velocity measurements were carried out only in the flow region between the inner wall and the radius of maximum velocity (*inner region*). The integration of the inner velocity profiles, experimentally obtained, enables a determination of the resistance coefficient law for the inner region f_1. This coefficient, as shown by Macagno and McDougall (1966) and Mossa and Petrillo (1995), is related to the average resistance coefficient f.

Revision received May 11, 2005/Open for discussion until June 30, 2007.

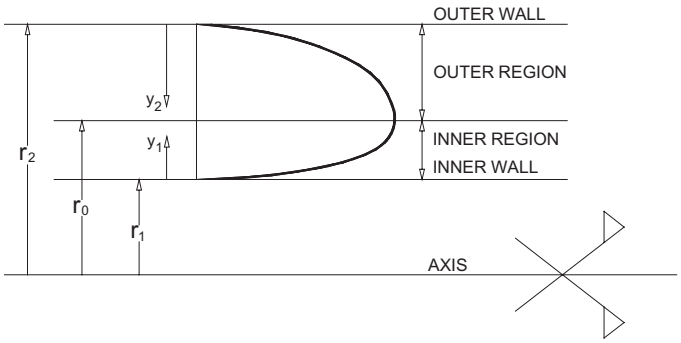

Figure 1 Definition sketch for flow in annular conduits.

1.1 Annular flow field characteristics

As proposed by Macagno and McDougall (1966) and in order to introduce general concepts, the assumed velocity distributions of turbulent flow will symbolically be expressed in the following way for the inner and outer regions, respectively (see Fig. 1)

$$\frac{u_1}{\sqrt{\tau_1/\rho}} = F_1\left(\frac{y_1}{y_1'}\right) \quad \text{for } r_1 \le r \le r_0 \tag{1}$$

$$\frac{u_2}{\sqrt{\tau_2/\rho}} = F_2\left(\frac{y_2}{y_2'}\right) \quad \text{for } r_0 \le r \le r_2 \tag{2}$$

where u_1 and u_2 are local mean velocities in the inner and outer regions, respectively; τ_1 and τ_2 are shear stresses at the inner and outer walls, respectively; y_1 and y_2 are distances from inner and outer walls, respectively; y_1' and y_2' are length scales, that will be better defined afterwards; r_1, r_2 and r_0 are radii of inner and outer walls and the radius at point of maximum velocity, respectively; ρ is water density; and $F_1$and F_2 are similarity functions representing the inner and outer velocity law, respectively.

Of course, at $r = r_0$, $u_1 = u_2$; therefore

$$\frac{\tau_1}{\tau_2} = \frac{F_2^2\left(\frac{r_2-r_0}{y_2'}\right)}{F_1^2\left(\frac{r_0-r_1}{y_1'}\right)} \tag{3}$$

is obtained for the ratio of absolute values of shear stresses at the walls.

An additional relationship involving these stresses results from the dynamic equations for fluid annular cylinders of unit length, one for each layer

$$\gamma J\pi\left(r_0^2 - r_1^2\right) = 2\pi r_1\tau_1, \quad \gamma J\pi\left(r_2^2 - r_0^2\right) = 2\pi r_2\tau_2 \tag{4}$$

where J is the slope of the head grade line and γ is water specific weight.

It has been assumed that the shear stress at $r = r_0$ is zero. Eliminating γJ between these two expressions, one finds the ratio of the wall shear stresses to be also given by

$$\frac{\tau_1}{\tau_2} = \frac{\left(r_0^2 - r_1^2\right)}{\left(r_2^2 - r_0^2\right)}\frac{r_2}{r_1}. \tag{5}$$

Using Eqs (3) and (5) r_0 may be calculated as long as F_1 and F_2 are known. Then, it is important to determine the overall resistance coefficient f or compute the local resistance coefficients f_1 and f_2 for the inner and outer regions.

The average value of the shear stresses of the walls is given by

$$\tau = \frac{\tau_1 r_1 + \tau_2 r_2}{r_1 + r_2}. \tag{6}$$

The resistance coefficients f, f_1 and f_2 are defined by means of

$$\tau = \rho f\frac{U^2}{8} = \gamma R J, \quad \tau_1 = \rho f_1\frac{U_1^2}{8} = \gamma R_1 J,$$
$$\tau_2 = \rho f_2\frac{U_2^2}{8} = \gamma R_2 J \tag{7}$$

in which U, U_1 and U_2 indicate the average velocities for the whole stream and for its inner and outer regions, respectively; R, R_1 and R_2 are the overall hydraulic radius and the hydraulic radii for the inner and outer regions, respectively

$$R = \frac{r_2 - r_1}{2}, \quad R_1 = \frac{r_0^2 - r_1^2}{2r_1}, \quad R_2 = \frac{r_2^2 - r_0^2}{2r_2}. \tag{8}$$

1.2 Hydraulically smooth flow

If both the inner and outer walls are hydraulically smooth, the velocity distribution, as proposed by Macagno and McDougall (1966), may be assumed

$$\frac{u_1}{u_{*1}} = A\ln\left(\frac{u_{*1}}{\nu}y_1\right) + B = a\,\log\left(\frac{u_{*1}}{\nu}y_1\right) + B,$$
$$\frac{u_2}{u_{*2}} = A\ln\left(\frac{u_{*2}}{\nu}y_2\right) + B = a\,\log\left(\frac{u_{*2}}{\nu}y_2\right) + B \tag{9}$$

which can also be expressed as

$$\frac{u_1}{u_{*1}} = A\ln\left(C\frac{u_{*1}}{\nu}y_1\right), \quad \frac{u_2}{u_{*2}} = A\ln\left(C\frac{u_{*2}}{\nu}y_2\right) \tag{10}$$

where $u_{*1} = \sqrt{\tau_1/\rho}$; $u_{*2} = \sqrt{\tau_2/\rho}$ are the friction velocities of the inner and outer walls, respectively; $A = 1/k$, B, C and $a = 2.30/k$ are empirical coefficients of the logarithmic law; k is Karman's parameter; and ν is water kinematic viscosity.

On this subject, Brighton and Jones (1964) have indicated modifications of the constants A and C of the logarithmic velocity distribution law, even if Macagno and McDougall observed that the values proposed by Brighton and Jones would leave them with unacceptable deviations with respect to the circular pipes, for which well-established constants are available.

These considerations point out the opportunity to make velocity measurements in annular conduits, especially in the inner region, where the wall is convex, to a better comprehension of the flow field.

Starting from Eq. (5) and taking into account Eq. (10), Macagno and McDougall (1966) proposed the following relation for r_0

$$\left[\frac{\beta^2 - \alpha^2}{\alpha(1-\beta^2)}\right]^{1/2} = \frac{\ln\left[\frac{C}{4\sqrt{2}}\left(\frac{1-\beta^2}{1-\alpha}\right)^{1/2}\left(\frac{1-\beta}{1-\alpha}\right)Re\sqrt{f}\right]}{\ln\left[\frac{C}{4\sqrt{2}}\left(\frac{\beta^2-\alpha^2}{\alpha(1-\alpha)}\right)^{1/2}\left(\frac{\beta-\alpha}{1-\alpha}\right)Re\sqrt{f}\right]} \tag{11}$$

where $Re = (4RU)/\nu$ is the overall Reynolds number and

$$\alpha = \frac{r_1}{r_2}, \quad \beta = \frac{r_0}{r_2}. \tag{12}$$

Macagno and McDougall assumed the coefficients A and C equal to the values for the circular conduits.

Doshi and Gill (1971) obtained a closed-form solution for the radius of maximum velocity in a simple manner by making some reasonable assumptions. It was found that

$$\beta^3 = \frac{\alpha}{2}(1+\alpha)\,. \tag{13}$$

Doshi and Gill compared Eq. (13) with the available experimental data and with the empirical expression of Kays and Leung (1963), which is

$$\beta = \frac{\alpha + \alpha^{0.343}}{1 + \alpha^{0.343}}. \tag{14}$$

The agreement of Eq. (13) with the experimental data was satisfactory, if we take into account the simplicity and closed-form of the equation. However, Doshi and Gill noted that at lower Reynolds numbers and for lower radius ratios, β is function not only of α but also of the Reynolds number. Nevertheless, the dependence of β on Re is very small as shown by Macagno and McDougall.

2 Experimental set-up

The set-up consists of a plexiglass circular conduit 205 cm long with a 150 mm diameter. Both ends are connected with a steel tube with 153 mm diameter. The upstream steel pipe is 10.50 m long, and the downstream one is 7.18 m long. The core of steel and plexiglass tubes is a smooth PVC tube with 60 mm outer diameter, centered and blocked through screws, positioned at several cross sections.

The experimental set-up is supplied by a closed hydraulic circuit of the laboratory consisting of an elevated reservoir with constant level supplied by a pump. The flow rate is controlled by two valves, positioned upstream and downstream of the system, and measured by a triangular weir. The head losses through 177 cm in the smooth plexiglass-PVC annular conduit were measured using a water differential manometer. Figure 2 shows a sketch of the experimental set-up.

The axial velocity components were measured, in the inner region, using an LDA system, which is composed of a 20 mW He–Ne laser generator, a DISA 55X Modular LDA Optics, a DISA 55N20 Doppler Frequency Tracker. This processor receives signals from the photomultiplier in forward scattering mode.

Refraction problems connected with the LDA system were solved as described by Mossa and Petrillo (1995).

To obtain the local mean velocity it was necessary to determine the suitable acquisition time for velocity samples, and the suitable interval time between two successive measured samples in order to obtain all the frequencies of turbulence.

Using a computer with an A/D electronic board of National Instruments (model AT-MIO 16 H), the mean velocity was obtained with 65,535 total samples; the data rate was equal to 200 Hz.

3 Analysis of experimental results

3.1 Axial mean velocity profiles

Measurements of velocity for different flow rates (from 2.00×10^{-3} to 5.98×10^{-3} m^3/s with corresponding Reynolds number equal to 10,404 to 29,472, respectively) were done. The summary of flow field data are reported in Table 1, where Q is the discharge, Re the average Reynolds number, τ_0 is the overall shear stress and τ_1 is the inner shear stress.

For this range of conditions, the maximum velocity occurs at distances between 18 and 19 mm from the inner wall. This result is in agreement with the law of the maximum velocity position proposed by Macagno and McDougall (1966) and Doshi and Gill (1971).

Figure 3 reports our result with the literature data published by Doshi and Gill.

The analysis of the local mean velocity distributions, using u_{*_1} as reference velocity and ν/u_{*_1} as reference length, was carried out. The figures are not reported for the sake of brevity.

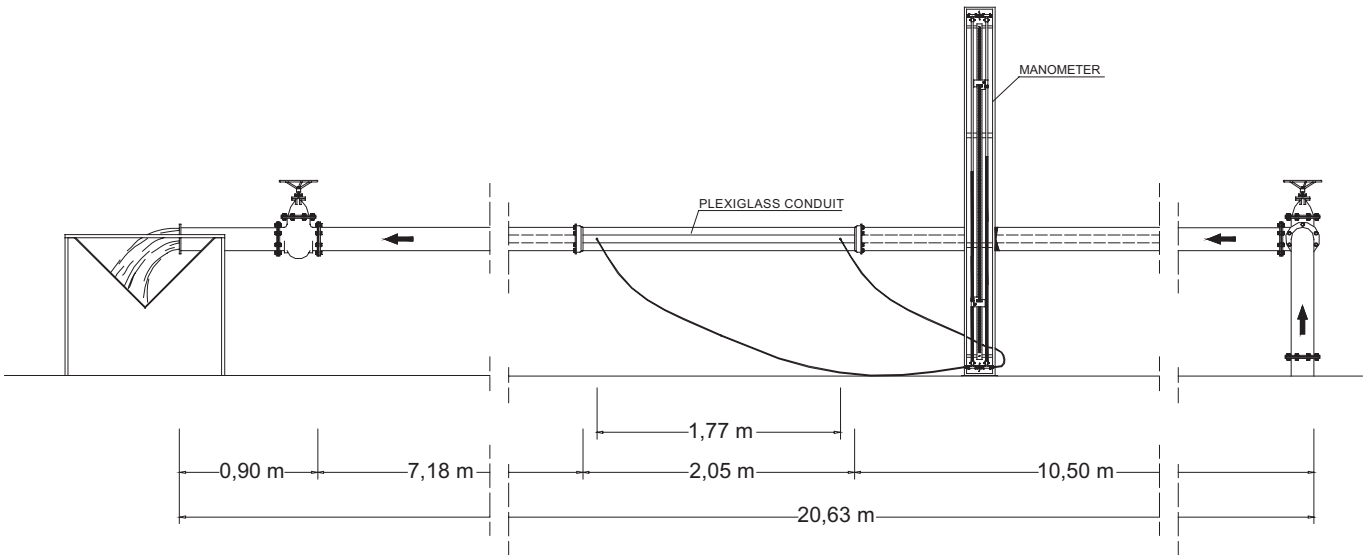

Figure 2 Sketch of the experimental set-up.

Table 1 Experimental configurations

No.	Q (m^3/s)	Re	U (m/s)	Water temperature (°K)	Overall shear stress, τ (N/m^2)	Inner shear stress, τ_1 (N/m^2)
1	2.00×10^{-3}	10,404	0.13	287.36	0.090	0.095
2	2.50×10^{-3}	13,313	0.17	288.26	0.132	0.140
3	3.02×10^{-3}	15,588	0.20	287.06	0.185	0.196
4	3.50×10^{-3}	17,877	0.24	286.66	0.240	0.254
5	3.96×10^{-3}	21,142	0.27	288.36	0.293	0.311
6	4.50×10^{-3}	23,902	0.30	288.16	0.365	0.387
7	5.15×10^{-3}	26,862	0.35	287.46	0.466	0.493
8	5.58×10^{-3}	28,275	0.38	286.36	0.539	0.571
9	5.98×10^{-3}	29,472	0.40	285.66	0.602	0.637

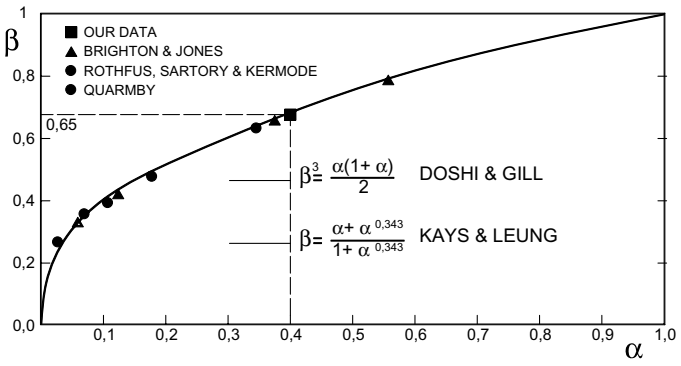

Figure 3 Variation of radius of maximum velocity with radius ratio.

Table 2 Parameters of velocity profiles

No.	k	B	Profile parameter, Π
1	0.411	5.76	0.177
2	0.404	5.70	0.143
3	0.381	5.25	0.115
4	0.387	5.00	0.158
5	0.389	5.00	0.117
6	0.390	5.28	0.142
7	0.377	4.92	0.104
8	0.385	5.16	0.102
9	0.418	6.21	0.118
Mean	0.394	5.36	0.131

From the analysis it is noted that the logarithmic region increases with Reynolds number. In particular, for the highest Re, the logarithmic region extends nearly between $y_1^+ = 15$ and $y_1^+ = 70$, while for the lowest Re it is valid for $27 < y_1^+ < 32$, where $y_1^+ = y_1 u_{*1}/\nu$.

Table 2 reports the experimental values of Karman's parameter k and the additive constant B of the logarithmic law, obtained using least square fits of the points which show a linear trend in the classic logarithmic region.

The mean value of k is 0.394 with standard deviation equal to 0.014, and the mean value of B is 5.36 with standard deviation equal to 0.43.

The values of these coefficients are close to the circular conduits cases.

It is well known that it is very difficult to get velocity measurements in the viscous sublayer because of the optical problem of laser beams and the noise level of the Doppler signal. The experimental data show clearly the existence of the well known transitional zone (*buffer layer*) connecting the viscous sublayer and logarithmic layer.

We investigated the external region (*outer layer*), where Coles (1956) and Marchi (1961) proposed similar corrective functions for the logarithmic velocity law.

The *wake function* proposed by Coles, which we tried to use in this study, is

$$W\left(\frac{y_1}{\delta}\right) = \frac{\Pi}{k} 2 \sin^2\left(\frac{\pi y_1}{2\delta}\right) \tag{15}$$

where δ is the distance from the inner wall to the position of maximum velocity and Π is the profile parameter.

The experiments show that the behavior of the velocity profiles in the outer layer is not similar to the circular pipe one, but it curved down nearly in the middle of the outer layer and cut the logarithmic regression line. Analogous results were observed by Nouri and Whitelaw (1994), who analyzed annular flows with and without rotation of the inner cylinder.

The velocity at the point of maximum deviation from the logarithmic law is not the maximum one. Therefore in our case, in order to calculate Π, we used δ' defined as the distance from the inner wall to the measurement point whose mean velocity presents the maximum deviation from the logarithmic law.

The values of profile parameter Π of all configurations are reported in Table 2; its mean value is equal to 0.131.

However, the wake function of Coles cannot describe the whole velocity profile of the outer layer, in agreement with the measurements of Nouri and Whitelaw (1994).

3.2 *Turbulence analysis*

The turbulence intensities u' were determined. Figure 4 reports the distribution of Kv (defined as the turbulence intensities u' nondimensionalized by the local mean velocity) against y_1^+.

This figure shows that Kv values from all runs collapse on a single curve with little scatter. We can conclude that Kv can be related with y_1^+. This means that in order to obtain a similarity curve, the relation has to include the effect of the wall shear stress.

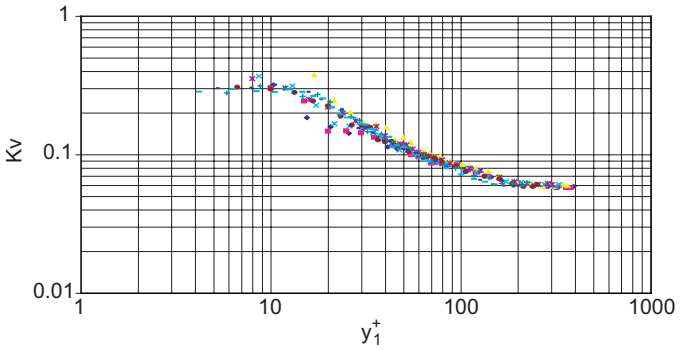

Figure 4 Turbulence index against y_1^+.

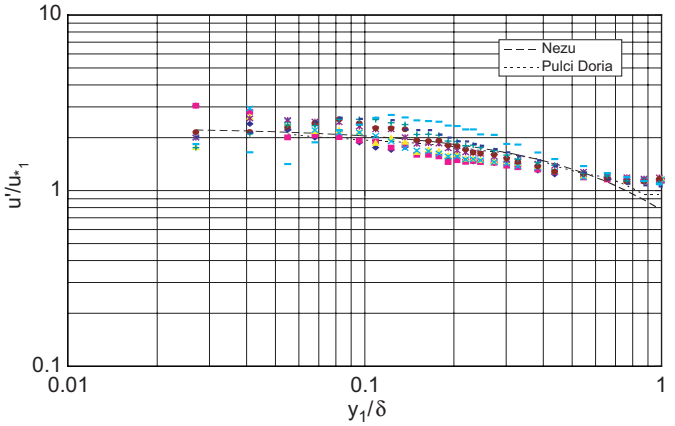

Figure 5 Dimensionless turbulence intensities against y_1/δ.

Figure 5 shows turbulence intensities u' nondimensionalized by friction velocity u_{*_1} against y_1/δ. The same picture reports two functions for turbulence intensities proposed by Nezu (1982) and Pulci Doria and Bottillo (1990).

It is noted that the two functions fit all data on the average, with the exception of the greater values of y_1/δ, which is the same zone where the experimental velocity profile is not in agreement with the wake function of Coles.

In order to study how velocity fluctuations are distributed around the local average value, statistical analysis was carried out. As mentioned before, mean velocities were obtained with enough total acquisition time to make the mean value constant with time. Therefore, the recorded velocity fluctuations can be assumed statistically steady.

Figure 6 reports skewness S against y_1^+ for all configurations. It is noted that S tend to decrease from the highest positive value with increasing y_1^+, until it reaches the minimum (negative) value at y_1^+ equal nearly to the value at which the logarithmic region starts.

In the outer layer, skewness tends to increase until it becomes nil at the position of maximum deviation from the logarithmic law. Then S takes small positive values.

Figure 7 reports kurtosis Kagainst y_1^+ for all configurations. The figure shows that kurtosis is equal to 3 (i.e. the Gaussian value) at nearly the same position where skewness is equal to 0 (i.e. the Gaussian value).

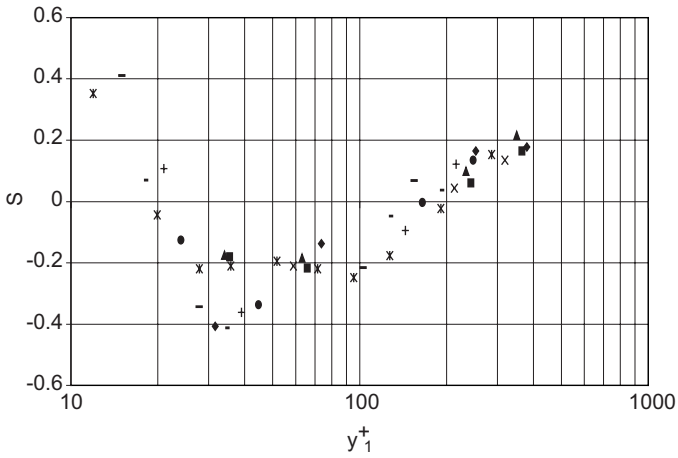

Figure 6 Skewness diagram.

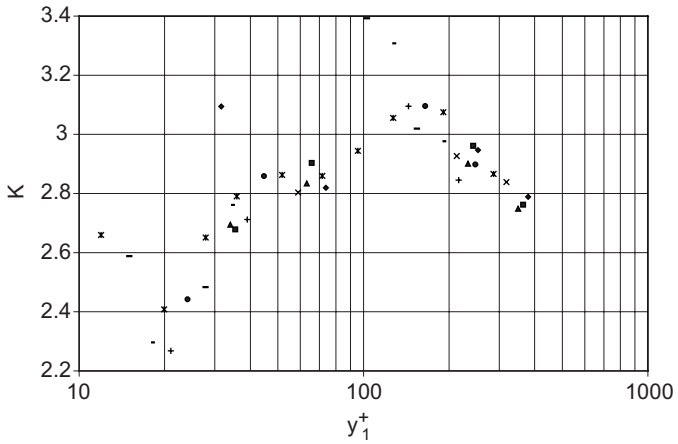

Figure 7 Kurtosis diagram.

The characteristics of skewness and kurtosis indicate that in the zone near the wall, where the influence of wall itself is remarkable and the shear stress is maximum, the distribution of velocity fluctuations is not Gaussian. In the outer layer the probability density distributions tends to become Gaussian.

Energy spectra were determined for several velocity series of experimental runs. According to the literature, the results show that there are two main regions for each spectrum described by two lines of different slopes. The slope of $-5/3$, which was predicted by Kolmogorov, is then replaced by a greater slope for greater frequencies.

For different distances from the inner wall, microscales (λ) and integral scales (I) of turbulence were calculated using the autocorrelation functions (A_c) of the velocity series:

$$\left.\frac{d^2 A_c}{dT^2}\right|_{T=0} = -\frac{2}{\lambda^2} \tag{16}$$

$$I = \int_0^\infty A_c(T)\,dT \tag{17}$$

where T is the lag time. Other methods, based on the cosine transform of the energy spectrum and the time derivative of the velocity components (Nalluri and Novak, 1973) were also employed to determine λ, obtaining the same results. It is known that the microscale λ is associated with the time scale of the smaller

eddies, which are responsible for energy dissipation. On the other hand, the integral time scale I is associated with the larger eddies. In turbulence, it is assumed that the integral scale is finite. The value of I is a rough measure of the interval over which $u_1(t)$ is correlated with itself.

The results were compared with the same scales calculated using power spectra. The calculated scales, which were analogous for both methods, are reported in Figs 8 and 9. From these figures it is clear that both micro and integral scales are greater for runs with lower Reynolds numbers.

Eddies contributing most to the dissipation of energy have a very small time scale compared to the time scale of the flow. The results of Fig. 9 suggest that small eddies tend to assume greater and greater frequencies, i.e. smaller and smaller time scales, for flows with greater Reynolds numbers. Physically, this means that in flows with greater Reynolds numbers small eddies can *better* dissipate energy.

In addition, the time interval over which fluctuating velocity is correlated with itself decreases with increasing Reynolds numbers.

These interesting aspects of the turbulent phenomena are well synthesized in Figs 8 and 9.

3.3 *Resistance coefficient*

Macagno and McDougall (1966) proposed the following relation for the overall resistance coefficient f

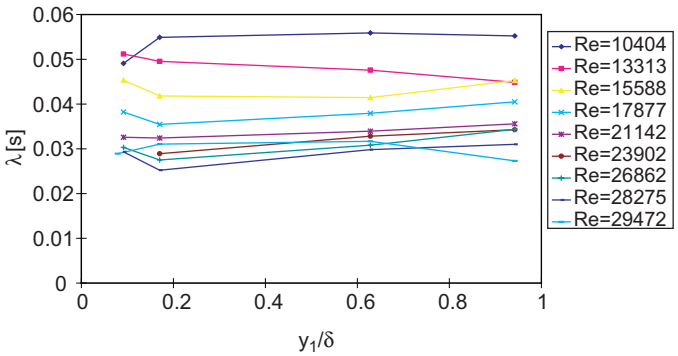

Figure 8 Microscales (λ) of turbulence.

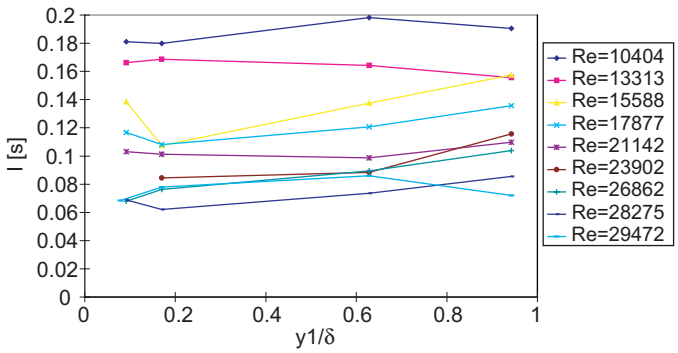

Figure 9 Integral scales (I) of turbulence.

$$\frac{1}{\sqrt{f}} = \frac{A}{4\sqrt{2}}\left[\frac{1-\beta^2}{1-\alpha}\right]^{1/2} \times \left\{2\ln\left[\frac{C}{4\sqrt{2}}\left(\frac{1-\beta^2}{1-\alpha}\right)^{1/2}\left(\frac{1-\beta}{1-\alpha}\right)Re\sqrt{f}\right] - \left[\frac{\beta^2-\alpha^2}{\alpha\left(1-\beta^2\right)}\right]^{1/2}\frac{\beta-\alpha}{1-\alpha^2}(3\alpha+\beta) - \frac{1-\beta}{1-\alpha^2}(3+\beta)\right\}. \tag{18}$$

As proposed by Mossa (1991) and Mossa and Petrillo (1995), to calculate f_1 and f_2 the following relations may be used

$$J = \frac{fU^2}{2g4R} = \frac{f_1U_1^2}{2g4R_1} = \frac{f_2U_2^2}{2g4R_2}. \tag{19}$$

The equality between the second and the third expressions of Eq. (19) may be written as follows

$$\frac{fU^2}{2g4\frac{r_2-r_1}{2}} = \frac{f_1U_1^2}{2g4\frac{r_0^2-r_1^2}{2r_1}} \tag{20}$$

that is

$$\frac{fU}{32R^2}\frac{Re\mu}{\gamma} = \frac{f_1U_1}{32R_1^2}\frac{Re_1\mu}{\gamma} \tag{21}$$

where

$$Re_1 = \frac{(4R_1U_1)}{\nu} \tag{22}$$

is the inner Reynolds number.

Equation (21) may be written as follows

$$\frac{fRe^2}{R^3} = \frac{f_1Re_1^2}{R_1^3} \tag{23}$$

that is

$$\frac{Re\sqrt{f}}{R^{3/2}} = \frac{Re_1\sqrt{f_1}}{R_1^{3/2}}. \tag{24}$$

Taking into account Eqs (8) and (12), relation (24) becomes

$$Re_1\sqrt{f_1} = \left[\frac{\beta^2-\alpha^2}{\alpha(1-\alpha)}\right]^{3/2}Re\sqrt{f}. \tag{25}$$

The analogous relation between f_2 and f is

$$Re_2\sqrt{f_2} = \left[\frac{1-\beta^2}{1-\alpha}\right]^{3/2}Re\sqrt{f} \tag{26}$$

where

$$Re_2 = \frac{(4R_2U_2)}{\nu} \tag{27}$$

is the outer Reynolds number.

It is possible to integrate the velocity law of the inner or outer layer in order to define a relation for f_1 or f_2, respectively, and then, using Eq. (25) or (26), to obtain the overall resistance coefficient f (see Mossa and Petrillo, 1995).

Of course Eq. (18) needs the constants A and C of Eq. (10), which Macagno and McDougall assumed to be exactly equal to the circular conduits cases. As written, Brighton and Jones

(1964) have indicated modifications of the constants A and C of the logarithmic velocity distribution law.

Neglecting the viscous sublayer and the wake function, it is possible to calculate the inner resistance coefficient, starting from the experimental velocity law of the inner region.

The following relation

$$\frac{U_1}{u_{*_1}} = \sqrt{\frac{8}{f_1}} = \frac{1}{\pi(r_0^2 - r_1^2)} \int_{r_1}^{r_0} \frac{u(r)}{u_{*1}} 2\pi r \, \mathrm{d}r \tag{28}$$

taking into account the first of Eq. (9), becomes

$$\frac{U_1}{u_{*_1}} = \frac{2\pi}{\pi(r_0^2 - r_1^2)} \int_{r_1}^{r_0} \left[B + \frac{1}{k} \ln\left(\frac{y_1 u_{*1}}{\nu}\right) \right] r \, \mathrm{d}r. \tag{29}$$

Changing the variables as follows

$$r = y_1 + r_1, \quad \mathrm{d}r = \mathrm{d}y_1 \tag{30}$$

from Eq. (29) and taking into account the relations (12), the expression for f_1 will be

$$\frac{1}{\sqrt{f_1}} = \frac{1}{\sqrt{8}} \left[B - \frac{1}{k} \frac{3\alpha + \beta}{2(\alpha + \beta)} + a \log \frac{2\alpha}{8\sqrt{2}(\alpha + \beta)} \right] + \frac{a}{\sqrt{8}} \log(Re_1 \sqrt{f_1}). \tag{31}$$

Referring to the values of α and β of the annular conduit analyzed in this study and the experimental mean values of a, B and k, Eq. (31) becomes

$$\frac{1}{\sqrt{f_1}} = 2.04 \log\left(\frac{Re_1 \sqrt{f_1}}{4.20}\right). \tag{32}$$

In Eq. (32) the constant 4.20 is present, instead of 2.51 for the Prandtl relation for resistance coefficient of circular conduits. This is the effect of the shape factor, that for Eq. (32) is related to the inner region of the annuli.

In this work we calculated the resistance coefficient of the smooth annular conduit for flow rates with *Re* between 10,404 and 275,920. These runs include the ones reported in Tables 1 and 2, for which velocity profiles were measured, and other configurations for which only the head grade line J was measured (see Mossa and Petrillo, 1995).

Figure 10 reports the experimental values of f and the ones calculated using equations of Macagno and McDougall (1966), Lorenz (1932) and Eqs (23) and (31) as proposed by Mossa and Petrillo (1995).

Theoretical values of f calculated using the Prandtl's relation for circular conduits are also reported.

From this figure, it is clear that for *Re* >100,000, the values of f obtained from different relations are quite similar.

On the contrary, for *Re* <100,000 the relation of Macagno and McDougall gives values of f smaller than the experimental ones, whereas the relation of Lorenz and the procedure proposed in this study gives values which fit better the experimental data. This behavior is similar to the one observed by Brighton and Jones (1964).

It is clear from Fig. 10 that experimental and calculated values of f for annular conduits are always a little higher than the ones of circular conduits.

4 Conclusions

The present paper reports the experimental study of turbulent flow in concentric smooth annular conduits developed at the Water Engineering and Chemistry Department of Bari Technical University (Italy).

From the velocity profiles, which were carried out for flows with $10,000 < Re < 30,000$, we noted that the logarithmic zone increases with increasing Reynolds numbers. The mean value of Karman's parameter k was equal to 0.394 and the mean value of the additive constant B of log-law was 5.36. They are close to the values for circular conduits.

Experimental data show clearly the existence of a transitional zone (*buffer layer*) connecting the viscous sublayer with the logarithmic layer.

The wake function for the annulus differed from that of the circular pipe. In fact, the deviation of the velocity profiles from the log-law reached its maximum value in the middle of the region of deflection and then decreased until it became nil. Here, the velocity profiles intercepted the log-law. The mean value of the profile parameter of Coles wake function (Π), calculated from the position of maximum deviation from the log-law, was equal on the average to 0.131.

The turbulent index (*Kv*), defined as the ratio of turbulence intensities and the local mean velocity, as general behavior, starts with the highest value near the wall; then it decreases to take constant value at the position of maximum velocity. Moreover, the distribution of *Kv* in the inner region goes up with decreasing *Re*. When the distributions of *Kv* are related to the dimensionless distance $y_1^+ = y_1 u_{*_1}/\nu$, all data, for all different Reynolds numbers, follow the same curve. This means that *Kv* is related with y_1^+ (i.e. the relation has to include the wall shear stress effect). The distribution of turbulence intensities nondimensionalized by friction velocity (u_{*_1}) was in agreement with the functions of Nezu (1982) and Pulci Doria and Bottillo (1990).

Measurements of velocity fluctuations were analyzed statistically. Probability density distributions for different positions were compared with the Gaussian distribution. Tools of comparison were coefficients of asymmetry (*skewness*) and flatness

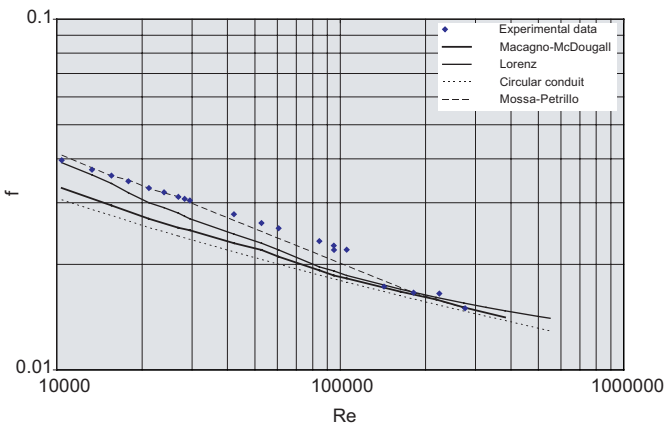

Figure 10 Resistance coefficients against Reynolds number.

(*kurtosis*). The results show that the probability density distributions are not Gaussian for velocity series measured near the wall. Particularly, in the logarithmic region, skewness reaches a maximum deviation from zero, which indicates the non-Gaussian behavior. The probability distributions tend to the Gaussian one at the measurement points with greater distance from the wall. In this zone both skewness and kurtosis assume Gaussian values.

For different distances from the inner wall micro and integral scales of turbulence were calculated. The results show that in flows with greater Reynolds numbers small eddies tends to assume greater and greater frequencies and that the time interval over which fluctuating velocity is correlated with itself becomes smaller and smaller.

The integration of the inner velocity profiles, experimentally obtained, enables a determination of the resistance coefficient law for the inner region (f_1). This one, as shown by Macagno and McDougall (1966) and Mossa and Petrillo (1995), is related to the average resistance coefficient f. Measurements of the losses in the annular pipe show that, for $Re < 100{,}000$, the resistance coefficients are always higher than the ones obtained by the Macagno and McDougall law. For $Re > 100{,}000$, all the analyzed methods are in substantial agreement with experimental data. Theoretical and experimental values of f in smooth annular pipe are always a little higher than the smooth circular pipe ones.

Notation

A = Coefficient in logarithmic velocity law
A_C = Autocorrelation function
B = Coefficient in logarithmic velocity law
C = Coefficient in logarithmic velocity law
f = Average resistance coefficient
f_1 = Resistance coefficient for inner wall
F_1 = Similarity function representing the inner velocity law
f_2 = Resistance coefficient for outer law
F_2 = Similarity function representing the outer velocity law
I = Turbulent integral scale
k = Karman's parameter in logarithmic velocity law
K = Kurtosis of $u_1(t)$
K_v = Turbulence index
r = Radial distance
R = Average hydraulic radius
r_1 = Radius of inner wall
R_1 = Hydraulic radius for inner layer
r_2 = Radius of outer wall
R_2 = Hydraulic radius for outer wall
Re = Average (overall) Reynolds number
Re_1 = Reynolds number for inner layer
Re_2 = Reynolds number for outer layer
S = Skewness of $u_1(t)$
T = Lag time
U = Average velocity for whole stream
u_{*_1} = Inner friction velocity
u_{*_2} = Outer friction velocity
u_1 = Local velocity in inner layer
U_1 = Average velocity for inner layer
u_2 = Local velocity in outer layer
U_2 = Average velocity for outer layer
u' = Turbulent intensities
W = Cole's wake function
y_1' = Inner length parameter of turbulent flow
y_2' = Outer length parameter of turbulent flow
$y_1^+ = y_1 u_{*_1}/\nu$ = Dimensionless distance from inner wall
y_1 = Distance from inner wall
y_2 = Distance from outer wall
α = Ratio of inner and outer radii
β = Relative distance from outer wall for velocity maximum point
γ = Water specific weight
δ = Distance from the inner wall to the position of maximum velocity
δ' = Distance from the inner wall to the measurement point whose mean velocity presents the maximum deviation from the logarithmic law
λ = Turbulent microscale
ν = Water kinematic viscosity
Π = Cole's profile parameter
ρ = Water density
τ = Average (overall) shear stress
τ_1 = Inner shear stress
τ_2 = Outer shear stress

References

1. BRIGHTON, J.A. and JONES, J.B. (1964). "Fully Developed Turbulent Flow in Annuli". *J. Basic Engng. Trans ASME* 86, 835–844.
2. CARDOSO, A.H., GRAF, W.H. and GUST, G. (1989). "Uniform Flow in a Smooth Open Channel". *J. Hydraul. Res. IAHR* 27(5), 603–616.
3. CENEDESE, A., COSTANTINI, A. and ROMANO, G.P. (1990). "Misure Simultanee Di tre componenti della velocità in uno strato limite turbolento mediante anemometria laser Doppler". *XXII Convegno di Idraulica e Costruzioni Idrauliche*, Cosenza, Italia, 4–7 October, Vol. 2, pp. 225–236 (in Italian).
4. COLES, D. (1956). "The Law of the Wake Function in the Turbulent Boundary Layers". *J. Fluid Mech.* 1, 191–226.
5. DOSHI, M.R. and GILL, W.N. (1971). "Fully Developed Turbulent Flow in an Annulus: Radius of Maximum Velocity". *J. Appl. Mech. Trans. ASME* 38(4), 1090–1091.
6. DURST, P., MELLING, A. and WHITELAW, J.H. (1976). *Principles and Practice of Laser-Doppler Anemometry.* Academic Press, London.
7. GENTILINI, B. (1935). "Sull'equazione del movimento uniforme delle correnti liquide". *L'Energia Elettrica (fasc. III)* XII, 161–178 (in Italian).

8. GHETTI, A. (1950). "Distribuzione delle velocità all'interno e sforzi di scorrimento al contorno nelle correnti a regime uniforme". *L'Energia Elettrica* XXVII(11–12), 664–681 (in Italian).
9. GRECO, M. and PULCI DORIA, G. (1983). "Strato limite in una corrente originariamente turbolenta". *Simposio sull'anemometria laser-Doppler nella sperimentazione idraulica*, Roma, 17–18 October (in Italian).
10. IDELCHIK, I.E. (1994). *Handbook of Hydraulic Resistance*. CRP Press, Boca Ratan, FL.
11. JONSSON, V.K. and SPARROW, E.M. (1966). "Experiments on Turbulent-Flow Phenomena in Eccentric Annular Ducts". *J. Fluid Mech.* 25(part I), 65–86.
12. KAYS, W.M. and LEUNG, E.Y. (1963) "Heat Transfer in Annular Passages—Hydrodinamically Developed Turbulent Flow with Arbitrarily Prescribed Heat Flux". *Int. J. Heat Mass Transfer* 6, 537–557.
13. LAMBERTI, A., PETRILLO, A. and RANIERI, M. (1983). "Phenomenological Study of Self-Aerated Flows on Smooth and Rough Channels Sloping up to 12°". *XX IAHR Congress*, Moscow 5–9 September, Vol. VI, pp. 238–248.
14. LORENZ, F.R. (1932), "Uber turbulente stromung durch rohre mit kreisring formigem querschnitt". *Mitt. Inst. fur Stromungsmaschinen Tech Hochschule Karlsruhe*, Helft, Vol. 2, pp. 26–66 (in German).
15. MACAGNO, E.O. and MCDOUGALL, D.W. (1966). "Turbulent Flow in Annular Pipes". *AIChE J.* 12(3), 437–444.
16. MARCHI, E. (1961). "Il moto uniforme delle correnti liquide nei condotti chiusi ed aperti". *L'Energia Elettrica* 4–5(part I), pp. 289–301; (part II); pp. 393–413 (in Italian).
17. MELLING, A. and WHITELAW, J.H. (1976). "Turbulent Flow in a Rectangular Duct". *J. Fluid Mech.* 78(part 2), 289–315.
18. MOSSA, M. (1991), "Diagrammi di velocità e resistenze al moto in condotti con sezione non circolare". Degree Thesis, Politecnico di Bari, Dipartimento di Ingegneria delle Acque, Bari, Italia (in Italian).
19. MOSSA, M. and PETRILLO, A. (1995). "Rilievi di velocità in condotti anulari". *III National Congress of A.I.VE.LA. (Italian Association of Laser Velocimetry)*, Ancona, Italia, 27–28 giugno, pp. 123–156 (in Italian).
20. NALLURI, C. and NOVAK, P. (1973). "Turbulence Characteristics in a Smooth Open Channel of Circular Cross-section". *J. Hydraul. Res. IAHR* 11(4), 343–368.
21. NEZU, I. (1982). "Turbulent Structure in Open-Channels Flows". PhD Thesis, Stanford University, California.
22. NOURI, J.M. and WHITELAW, J.H. (1994). "Flow of Newtonian and Non-Newtonian Fluids in a Concentric Annulus with Rotation of the Inner Cylinder". *J. Fluids Engng. Trans. ASME* 116, 821–827.
23. PULCI DORIA, G. and BOTTILLO, B. (1990). "La distribuzione delle intensità di turbolenza in correnti di varia natura". *XXII Convegno di Idraulica e Costruzioni Idrauliche*, Cosenza, Italia, 4–7 October, Vol. 2, pp. 33–43 (in Italian).
24. QUARMBY, A. (1967). "An Experimental Study of Turbulent Flow Through Concentric Annuli". *Int. J. Mech. Sci.* 9, 205–221.
25. ROTHFUS, R.R., SARTORY, W.K. and KERMODE, R.I. (1966). "Flow in Concentric Annuli at High Reynolds Numbers". *AIChE J.* 12, 1086–1091.
26. SHANDS, J., ALFREDSSON, H. and LINDGREN, E.R. (1980). "Annular Pipe Flow Subject to Axial Motion of the Inner Boundary". *Phys. Fluids* 23(10), 2144–2145.
27. SHARMA, B.I., LAUNDER, B.E. and SCOTT, C.J. (1976). "Computation of Annular, Turbulent Flow with Rotating Core Tube". *J. Fluids Engng. Trans. ASME* 98, 753–758.